

# Mixed partial-wave scattering with spin-orbit coupling and validity of pseudo-potentials

Xiaoling Cui

*Institute for Advanced Study, Tsinghua University, Beijing, 100084  
Department of Physics, Ohio State University, Columbus, OH 43210*

(Dated: November 9, 2018)

We present exact solutions of two-body problem for spin-1/2 fermions with isotropic spin-orbit(SO) coupling and interacting with an arbitrary short-range potential. We find that in each partial-wave scattering channel, the parametrization of two-body wavefunction at short inter-particle distance depends on the scattering amplitudes of all channels. This reveals the mixed partial-wave scattering induced by SO couplings. By comparing with results from a square-well potential, we investigate the validity of original pseudo-potential models in the presence of SO coupling. We find the s-wave pseudo-potential provides a good approximation for low-energy solutions near s-wave resonances, given the length scale of SO coupling much longer than the potential range. However, near p-wave resonance the p-wave pseudo-potential gives low-energy solutions that are qualitatively different from exact ones, based on which we conclude that the p-wave model can not be applied to the fermion system if the SO coupling strength is larger or comparable to the Fermi momentum.

## I. INTRODUCTION

Two-body problem takes the most fundamental place in the process of exploring and understanding many-body properties. In particular, two-body solutions determine the essential interaction parameter in the microscopic many-body Hamiltonian. In the field of dilute ultracold atoms, the two-body interaction is generally formulated by the zero-range pseudo-potential, provided that it produces the same asymptotic two-body wavefunction at length scale much shorter than the mean inter-particle distance but longer than the range of realistic potential. The generalized pseudo-potentials for all partial-waves were first derived by Huang and Yang[1], and then improved later by Stock *et al* [2]. So far the most popular pseudo-potential is in s-wave channel described by a single s-wave scattering length, which can be improved by including the energy-dependence in a self-consistent way[2, 3]. Another popular one is the p-wave pseudo-potential, described by the p-wave scattering volume which generally has strong energy-dependence[4, 5].

In view of the great success when applying pseudo-potential models to the homogenous or trapped atomic gases, it is generally believed that this model will equally apply to other configurations, such as in the presence of spin-orbit(SO) coupling. Recently, by sophisticated manipulations of laser field and magnetic field, the NIST group has successfully realized an optically synthesized magnetic field for ultracold neutral atoms[6]. As a result, an effective SO coupling is generated in the system along one direction. Subsequently there are several theoretical proposals to realize the symmetric Rashba SO coupling[7], and it is conceivable that an arbitrary type SO coupling could be achieved in future experiments. As usual, all existing theoretical studies about the SO coupled system are carried out in the framework of s-wave pseudo-potential, i.e., using the s-wave scattering length as that without SO coupling(see recent review [8]). Based on this model, the most remarkable effect of symmetric

SO coupling is to support a two-body bound state with an arbitrarily weak interaction, due to the modified low-energy density of state[9].

Although pseudo-potentials have been justified under confinement potentials[2, 3, 5], it is not obvious that it is still robust under the single-particle potential as special as SO couplings. In the two-body scattering process, trapping potentials and SO couplings have the same effect in mixing different partial-waves, either due to the trap anisotropy[10, 11], or due to the intermediate coupling with spin sector. However, unlike the trapping potentials, which generally contribute a trivial constant potential as two particles get close, the SO coupling intrinsically affects the kinetic term and thus still mix all partial-waves for the two-body wavefunctions at short inter-particle distance. This non-trivial effect is expected to have important influence on the validity of original pseudo-potentials in the presence of SO coupling. For instance, an obvious deficiency of original s-wave pseudo-potential is that this model can predict arbitrarily deep bound state with the binding energy scaled in terms of the SO coupling strength[9]; however, under a square-well (attractive) interaction potential the true binding energy must be lower-bounded by the potential depth. Moreover, this discrepancy can not be amended by taking into account the energy-dependence of s-wave scattering length, as we shall show later in Section IV.

In this paper, we make efforts to exactly solve the two-body problem with SO coupling for a general short-range interaction potential, without resorting to pseudo-potential models. For simplicity but without the loss of essence, we have chosen the isotropic SO coupling and studied in the subspace where only s-wave and p-wave scatterings are relevant. We show that the short-range parametrization of the wavefunction in each partial-wave channel will additionally rely on the scattering amplitude of another partial-wave channel, which reflects the mixed scattering between different orbital channels induced by SO coupling. The exact form of wavefunction obtained

above allows us to solve the two-body problem under a square-well interacting potential. By comparing with results from s-wave or p-wave pseudo-potentials, we address the validity of the latter in the presence of isotropic SO coupling. We find the s-wave pseudo-potential provides a good approximation for the low-energy scattering state and bound state solutions near s-wave resonance, with the correction depending on the strength of SO coupling, the finite range of the potential and contributions from p-wave channel. However, near p-wave resonance, using the p-wave pseudo-potential alone will lead to results that are qualitatively different from exact solutions from the square-well potential. We conclude that the p-wave pseudo-potential can not be applied to fermion system if the SO coupling strength is larger or comparable to the Fermi momentum. We shall address the underlying reasons for these results.

The rest of the paper is organized as follows. In section II, we present the exact solution for two spin-1/2 fermions under a general short-range interaction potential and with isotropic SO coupling. In section III we reduce the exact solutions to the framework of original s-wave and p-wave pseudo-potentials. In section IV we present the numerical results for two-body problem under the square-well potential, from which we address the validity of s-wave and p-wave pseudo-potential models. We summarize the paper in the last section.

## II. TWO-BODY PROBLEM WITH ISOTROPIC SPIN-ORBIT COUPLING

In this section we shall solve the two-body scattering problem for a special case of isotropic SO coupling. Assuming a general form of short-range interaction potential (See Eq.25), we obtain the wavefunction of scattering state (Eq.33) and analyze its long-range and short-range asymptotic behaviors. Particularly we show that its short-range behavior is parameterized by scattering amplitudes in all relevant partial-wave channels (Eqs.41,42). Finally we present the bound state solutions which can be deduced from scattering state solutions via Eq.43.

We start from the single-particle Hamiltonian of spin-1/2( $\uparrow, \downarrow$ ) fermions with isotropic SO coupling, (we set the reduced Planck constant  $\hbar = 1$ )

$$H_1 = \frac{\mathbf{k}^2}{2m} + \frac{\lambda}{m} \mathbf{k} \cdot \boldsymbol{\sigma} + \frac{\lambda^2}{2m}, \quad (1)$$

where  $\mathbf{k} = (k_x, k_y, k_z)$  and  $\boldsymbol{\sigma} = (\sigma_x, \sigma_y, \sigma_z)$  respectively denote the momentum operator and Pauli spin operator;  $\lambda$  is the strength of SO coupling. The single-particle eigen-state has two orthogonal branches as

$$\begin{aligned} |\mathbf{k}^{(+)}\rangle &= u_{\mathbf{k}}^{(+)} |\mathbf{k}_{\uparrow}\rangle + u_{\mathbf{k}}^{(-)} e^{i\phi_{\mathbf{k}}} |\mathbf{k}_{\downarrow}\rangle, \\ |\mathbf{k}^{(-)}\rangle &= -u_{\mathbf{k}}^{(-)} e^{-i\phi_{\mathbf{k}}} |\mathbf{k}_{\uparrow}\rangle + u_{\mathbf{k}}^{(+)} |\mathbf{k}_{\downarrow}\rangle; \end{aligned} \quad (2)$$

with  $\phi_{\mathbf{k}} = \arg(k_x + ik_y)$ ,  $u_{\mathbf{k}}^{(\pm)} = \sqrt{\frac{1}{2} \pm \frac{k_z}{2|\mathbf{k}|}}$ , and the corresponding eigen-energy  $\epsilon_{\mathbf{k}}^{(\pm)} = (|\mathbf{k}| \pm \lambda)^2 / (2m)$  as shown in Fig.1. Due to the isotropy of SO coupling, the total

angular momentum  $\mathbf{j} = \mathbf{l} + \mathbf{s}$  ( $\mathbf{s} = \frac{1}{2}\boldsymbol{\sigma}$ ) is conserved by  $H_1$ , giving the highest rotation symmetry among all types of SO couplings.

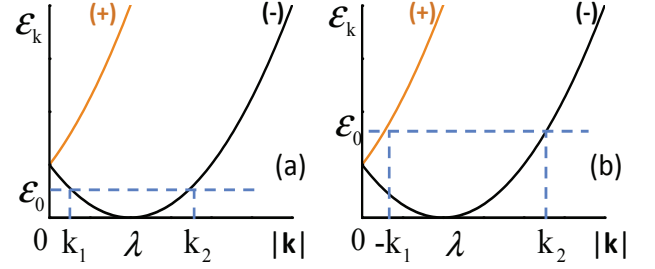


FIG. 1: (Color online) Single-particle spectrum,  $\epsilon_{\mathbf{k}}^{(\pm)} = (|\mathbf{k}| \pm \lambda)^2 / (2m)$ , with isotropic SO coupling. For given energy  $\epsilon_0 = k_0^2 / (2m)$ , two magnitudes of momentum are available as  $|k_1|$  and  $k_2$ , with  $k_1 = \lambda - k_0$ ,  $k_2 = \lambda + k_0$ .  $k_0 < \lambda$  in (a) and  $k_0 > \lambda$  in (b).

The two-particle Hamiltonian can be written as  $H_2 = H_{\mathbf{K}} + H_{\mathbf{k}}$ , with  $H_{\mathbf{K}}$  and  $H_{\mathbf{k}}$  respectively describing the center-of-mass motion with total momentum  $\mathbf{K} = \mathbf{k}_1 + \mathbf{k}_2$  and relative motion with momentum  $\mathbf{k} = (\mathbf{k}_2 - \mathbf{k}_1)/2$ ,

$$H_{\mathbf{K}} = \frac{\mathbf{K}^2}{4m} + \frac{\mathbf{K}}{4m} \cdot (I_1 \otimes \boldsymbol{\sigma}_2 + \boldsymbol{\sigma}_1 \otimes I_2), \quad (3)$$

$$H_{\mathbf{k}} = \frac{\mathbf{k}^2}{m} + \frac{\mathbf{k}}{m} \cdot (I_1 \otimes \boldsymbol{\sigma}_2 - \boldsymbol{\sigma}_1 \otimes I_2) + \frac{\lambda^2}{m}. \quad (4)$$

With isotropic SO coupling, the total angular momentum for two particles  $\mathbf{J} = \mathbf{L} + \mathbf{S}$  is also conserved, with  $\mathbf{L} = \mathbf{l}_1 + \mathbf{l}_2$ ,  $\mathbf{S} = \mathbf{s}_1 + \mathbf{s}_2$  respectively the total orbital angular momentum and total spin of particle 1 and 2. Moreover,  $\mathbf{L}$  can be decomposed as  $\mathbf{L} = \mathbf{L}_r + \mathbf{L}_R$ , with  $\mathbf{L}_r$  ( $\mathbf{L}_R$ ) the angular momentum for the relative motion  $\mathbf{r} = \mathbf{r}_2 - \mathbf{r}_1$  (center-of-mass  $\mathbf{R} = (\mathbf{r}_1 + \mathbf{r}_2)/2$ ). In view of the symmetry of  $H_2$ , in this paper we consider the scattering problem in the subspace of  $\mathbf{K} = 0$  ( $\mathbf{L}_R = 0$ ) and  $\mathbf{J} = \mathbf{L}_r + \mathbf{S} = 0$ . (The method presented below can be generalized to the case of non-zero  $\mathbf{K}$  or  $\mathbf{J}$ ).

For total  $\mathbf{K} = 0$ , the scattered wavefunction only depends on the relative coordinate  $\mathbf{r}$ , and is given by the Lippmann-Schwinger equation[12] as

$$\langle \mathbf{r} | \Psi_{\mathbf{k}} \rangle = \langle \mathbf{r} | \Psi_{\mathbf{k}}^{(0)} \rangle + \int d\mathbf{r}' \langle \mathbf{r} | G(E) | \mathbf{r}' \rangle \langle \mathbf{r}' | U | \Psi_{\mathbf{k}} \rangle. \quad (5)$$

where  $G(E) = \frac{1}{E - H_2 + i\delta}$  is the two-particle green function,  $U$  is the interaction operator;  $|\Psi_{\mathbf{k}}^{(0)}\rangle$  is the incident two-particle state with relative momentum  $\mathbf{k}$ , which can be either of the following three states

$$|\Phi_{\mathbf{k}}^{(--)}\rangle = |\mathbf{k}^{(-)}, -\mathbf{k}^{(-)}\rangle (-e^{i\phi_{\mathbf{k}}}), \quad (6)$$

$$|\Phi_{\mathbf{k}}^{(++)}\rangle = |\mathbf{k}^{(+)}, -\mathbf{k}^{(+)}\rangle (-e^{-i\phi_{\mathbf{k}}}), \quad (7)$$

$$|\Phi_{\mathbf{k}}^{(-+)}\rangle = |\mathbf{k}^{(-)}, -\mathbf{k}^{(+)}\rangle; \quad (8)$$

in coordinate space they are (we set the volume  $V = 1$  for normalization)

$$\langle \mathbf{r} | \Phi_{\mathbf{k}}^{(-)} \rangle = \frac{1}{\sqrt{2}} \left\{ -i \sin(\mathbf{k} \cdot \mathbf{r}) \left[ -\frac{k_-}{k} | \uparrow \uparrow \rangle + \frac{k_+}{k} | \downarrow \downarrow \rangle + \frac{k_z}{k} (| \uparrow \downarrow \rangle + | \downarrow \uparrow \rangle) \right] + \cos(\mathbf{k} \cdot \mathbf{r}) (| \uparrow \downarrow \rangle - | \downarrow \uparrow \rangle) \right\}, \quad (9)$$

$$\langle \mathbf{r} | \Phi_{\mathbf{k}}^{(++)} \rangle = \frac{1}{\sqrt{2}} \left\{ i \sin(\mathbf{k} \cdot \mathbf{r}) \left[ -\frac{k_-}{k} | \uparrow \uparrow \rangle + \frac{k_+}{k} | \downarrow \downarrow \rangle + \frac{k_z}{k} (| \uparrow \downarrow \rangle + | \downarrow \uparrow \rangle) \right] + \cos(\mathbf{k} \cdot \mathbf{r}) (| \uparrow \downarrow \rangle - | \downarrow \uparrow \rangle) \right\}, \quad (10)$$

$$\langle \mathbf{r} | \Phi_{\mathbf{k}}^{(-+)} \rangle = -\frac{1}{\sqrt{2}} i \sin(\mathbf{k} \cdot \mathbf{r}) \left\{ \left( 1 - \frac{k_z}{k} \right) e^{-i\phi_{\mathbf{k}}} | \uparrow \uparrow \rangle + \left( 1 + \frac{k_z}{k} \right) e^{i\phi_{\mathbf{k}}} | \downarrow \downarrow \rangle + \frac{k_{\perp}}{k} (| \uparrow \downarrow \rangle + | \downarrow \uparrow \rangle) \right\}; \quad (11)$$

with  $k = |\mathbf{k}|$ ,  $k_{\perp} = \sqrt{k_x^2 + k_y^2}$ ,  $k_{\pm} = k_x \pm i k_y$ .

Furthermore, the subspace of  $\mathbf{J} = \mathbf{L}_{\mathbf{r}} + \mathbf{S} = 0$  can be spanned by two orthogonal components as (labeled by  $|L_r, S; m_L, m_s\rangle$ )

$$|J=0\rangle_0 = |00; 00\rangle, \quad (12)$$

$$|J=0\rangle_1 = \frac{1}{\sqrt{3}} [|11; -1, 1\rangle + |11; 1, -1\rangle - |11; 0, 0\rangle] \quad (13)$$

Here  $|J=0\rangle_0$  is the spin-singlet combined with s-wave orbital channel, and  $|J=0\rangle_1$  is the spin-triplet combined with p-wave orbital channel. Now any state projected to  $J=0$  subspace can be written as

$$\langle \mathbf{r} | \Psi_{\mathbf{k}} \rangle_{J=0} = \psi_0(r) \langle \Omega_r | J=0 \rangle_0 + \psi_1(r) \langle \Omega_r | J=0 \rangle_1 \quad (14)$$

with bases

$$\langle \Omega_r | J=0 \rangle_0 = Y_{00}(\Omega_r) \frac{| \uparrow \downarrow \rangle - | \downarrow \uparrow \rangle}{\sqrt{2}}, \quad (15)$$

$$\begin{aligned} \langle \Omega_r | J=0 \rangle_1 &= \frac{1}{\sqrt{3}} [Y_{1,-1}(\Omega_r) | \uparrow \uparrow \rangle + Y_{11}(\Omega_r) | \downarrow \downarrow \rangle \\ &\quad - Y_{10}(\Omega_r) \frac{| \uparrow \downarrow \rangle + | \downarrow \uparrow \rangle}{\sqrt{2}}], \end{aligned} \quad (16)$$

and wavefunctions

$$\psi_0(r) = \int d\Omega_r \langle J=0 | \Omega_r \rangle \langle \mathbf{r} | \Psi_{\mathbf{k}} \rangle; \quad (17)$$

$$\psi_1(r) = \int d\Omega_r \langle J=0 | \Omega_r \rangle \langle \mathbf{r} | \Psi_{\mathbf{k}} \rangle. \quad (18)$$

Here  $\Omega_r$  denotes the azimuthal angle of relative coordinate  $\mathbf{r}$ , and  $Y_{lm}$  the spherical harmonics with azimuthal quantum numbers  $(l, m)$ . After projected, the eigenstates of  $H_2$ , i.e., Eqs.(9,10,11), are given by

$$\langle \mathbf{r} | \Phi_{\mathbf{k}}^{(-)} \rangle_{J=0} = \sqrt{4\pi} [j_0(kr) \langle \Omega_r | J=0 \rangle_0 + i j_1(kr) \langle \Omega_r | J=0 \rangle_1], \quad (19)$$

$$\langle \mathbf{r} | \Phi_{\mathbf{k}}^{(++)} \rangle_{J=0} = \sqrt{4\pi} [j_0(kr) \langle \Omega_r | J=0 \rangle_0 - i j_1(kr) \langle \Omega_r | J=0 \rangle_1], \quad (20)$$

$$\langle \mathbf{r} | \Phi_{\mathbf{k}}^{(-+)} \rangle_{J=0} = 0. \quad (21)$$

with  $j_l(x)$  ( $l=0,1$ ) the spherical Bessel function of  $l$ -th order. Particularly, Eq.21 shows that  $(-+)$  channel is not involved in the subspace of  $J=0$ .

Due to the single-particle spectrum modified by isotropic SO coupling (see Fig.1), the incident state of two particles with energy  $E = k^2/m$  can be an arbitrary combination of plane-waves with two different magnitudes of momenta,  $|\mathbf{k}_2| = \lambda + k$  and  $|\mathbf{k}_1| = |\lambda - k|$ . For  $k < \lambda$ ,

$$\langle \mathbf{r} | \Psi_{\mathbf{k}}^{(0)} \rangle_{J=0} = \alpha \langle \mathbf{r} | \Phi_{\mathbf{k}_2}^{(-)} \rangle_{J=0} + \beta \langle \mathbf{r} | \Phi_{\mathbf{k}_1}^{(-)} \rangle_{J=0}; \quad (22)$$

and for  $k > \lambda$ ,

$$\langle \mathbf{r} | \Psi_{\mathbf{k}}^{(0)} \rangle_{J=0} = \alpha \langle \mathbf{r} | \Phi_{\mathbf{k}_2}^{(-)} \rangle_{J=0} + \beta \langle \mathbf{r} | \Phi_{\mathbf{k}_1}^{(++)} \rangle_{J=0}; \quad (23)$$

which both result in  $(k_2 \equiv \lambda + k, k_1 \equiv \lambda - k)$

$$\langle \mathbf{r} | \Psi_{\mathbf{k}}^{(0)} \rangle_{J=0} = \sqrt{4\pi} \{ [\alpha j_0(k_2 r) + \beta j_0(k_1 r)] \langle \Omega_r | J=0 \rangle_0 + i [\alpha j_1(k_2 r) + \beta j_1(k_1 r)] \langle \Omega_r | J=0 \rangle_1 \}. \quad (24)$$

In view of the property of  $H_2$ , we also project the interaction  $U$  (with range  $r_0$ ) to  $J=0$  subspace as

$$\langle \mathbf{r} | U | \Psi_{\mathbf{k}} \rangle_{J=0} = \sqrt{4\pi} [F_0(r) \langle \Omega_r | J=0 \rangle_0 + F_1(r) \langle \Omega_r | J=0 \rangle_1], \quad (r < r_0) \quad (25)$$

here  $F_0, F_1$  denote the scattering amplitude in s-wave ( $L_{\mathbf{r}} = 0$ ) and p-wave ( $L_{\mathbf{r}} = 1$ ) channel. The Green function in Eq.5 is calculated by inserting a complete set of intermediate states (Eq.19 and 20),

$$\langle \mathbf{r} | G | \mathbf{r}' \rangle_{J=0} = \frac{1}{2} \sum_{\mathbf{k}} \left\{ \frac{\langle \mathbf{r} | \Phi_{\mathbf{k}}^{(-)} \rangle \langle \Phi_{\mathbf{k}}^{(-)} | \mathbf{r}' \rangle}{E - 2\epsilon_{\mathbf{k}}^{(-)} + i\delta} + \frac{\langle \mathbf{r} | \Phi_{\mathbf{k}}^{(++)} \rangle \langle \Phi_{\mathbf{k}}^{(++)} | \mathbf{r}' \rangle}{E - 2\epsilon_{\mathbf{k}}^{(+)} + i\delta} \right\}_{J=0}. \quad (26)$$

Here the prefactor 1/2 is to eliminate the double counting of inserted states.

Combining Eqs.(5, 24, 25, 26), we obtain the closed form of scattered wavefunction (for  $r > r_0$ ) in each partial-wave channel (see Eq.14) as

$$\begin{aligned}\psi_0/\sqrt{4\pi} &= \alpha j_0(k_2 r) + C_{k_2}[n_0(k_2 r) - i j_0(k_2 r)] + \beta j_0(k_1 r) + C_{k_1}[n_0(k_1 r) + i j_0(k_1 r)], \\ \psi_1/(i\sqrt{4\pi}) &= \alpha j_1(k_2 r) + C_{k_2}[n_1(k_2 r) - i j_1(k_2 r)] + \beta j_1(k_1 r) + C_{k_1}[n_1(k_1 r) + i j_1(k_1 r)]\end{aligned}\quad (27)$$

where ( $q = k_1$  or  $k_2$ )

$$C_q = \frac{q^2}{2(q-\lambda)}(f_0(q) - i f_1(q)), \quad (28)$$

$$f_0(q) = m \int_0^{r_0} dr r^2 F_0(r) j_0(qr), \quad (29)$$

$$f_1(q) = m \int_0^{r_0} dr r^2 F_1(r) j_1(qr), \quad (30)$$

and  $n_l(x)$  ( $l = 0, 1$ ) the spherical Neumann function of  $l$ -th order.

We further simplify the complex wavefunction (27) by employing the time-reversal symmetry, i.e.,  $[H_2, T] = 0$  where  $T$  is the time-reversal operator. Therefore we choose the wavefunction to be the eigen-state for both  $H_2$  and  $T$ . Noting that  $T\langle\Omega_r|J=0\rangle_0 = \langle\Omega_r|J=0\rangle_0$ ,  $T\langle\Omega_r|J=0\rangle_1 = -\langle\Omega_r|J=0\rangle_1$ , the only way to achieve  $T\Psi = e^{i\theta}\Psi$  is to assume

$$C_{k_2} = -\alpha \sin \delta e^{i\delta}, \quad (31)$$

$$C_{k_1} = \beta \sin \delta e^{i\delta}, \quad (32)$$

with  $\delta = \theta/2$ . Then up to a prefactor  $\sqrt{4\pi} \cos \delta e^{i\delta}$ , Eq.27 is reduced to

$$\begin{aligned}\psi_0 &= \alpha[j_0(k_2 r) - \tan \delta n_0(k_2 r)] + \\ &\quad \beta[j_0(k_1 r) + \tan \delta n_0(k_1 r)], \\ \psi_1/i &= \alpha[j_1(k_2 r) - \tan \delta n_1(k_2 r)] + \\ &\quad \beta[j_1(k_1 r) + \tan \delta n_1(k_1 r)].\end{aligned}\quad (33)$$

To this end we have obtained the exact form of scattered wavefunction for a given short-range potential  $U(\mathbf{r})$  defined in Eq.25. Eq.33 reveals a unique scattering property in the presence of isotropic SO coupling, i.e., the wavefunction in each partial-wave channel is characterized by two different momenta (see also Fig.1) with opposite phase shifts. Note that without SO coupling,  $\lambda = 0$ ,  $k_2 = -k_1 = k$ , Eq.33 reduces to the standard form of s-wave and p-wave scattered wavefunctions in free space.

The scattered wavefunction (Eq.33) has the following asymptotic behaviors at long-range and short-range of inter-particle distances. As  $kr \rightarrow \infty$ , the long-range behavior is (up to a prefactor  $\sqrt{4\pi} e^{i\delta}$ )

$$\psi_0 = \alpha \frac{\sin(k_2 r + \delta)}{k_2 r} + \beta \frac{\sin(k_1 r - \delta)}{k_1 r}, \quad (34)$$

$$\psi_1/i = \alpha \frac{\sin(k_2 r - \pi/2 + \delta)}{k_2 r} + \beta \frac{\sin(k_1 r - \pi/2 - \delta)}{k_1 r} \quad (35)$$

At short-range  $r_0 < r \ll 1/k$ , we have (up to a prefactor  $\sqrt{4\pi} \cos \delta e^{i\delta}$ )

$$\psi_0 = \alpha + \beta + \left(\frac{\alpha}{k_2} - \frac{\beta}{k_1}\right) \frac{\tan \delta}{r}, \quad (36)$$

$$\psi_1/i = \frac{\alpha k_2 + \beta k_1}{3} r + \left(\frac{\alpha}{k_2^2} - \frac{\beta}{k_1^2}\right) \frac{\tan \delta}{r^2}. \quad (37)$$

For simplicity, we consider the limit of zero-range potential, i.e., assuming  $F_i(r) \equiv \frac{\delta(r)}{4\pi r^2} \bar{F}_i(r \rightarrow 0)$  ( $i = 0, 1$ ) in Eq.25. Further according to Eqs.(29,30) we introduce

$$\bar{f}_0 = \frac{m}{4\pi} \bar{F}_0(r \rightarrow 0), \quad \bar{f}_1 = \frac{m}{4\pi} \frac{r \bar{F}_1(r \rightarrow 0)}{3} \Big|_{r \rightarrow 0}, \quad (38)$$

which gives  $f_0(q) = \bar{f}_0$ ,  $f_1(q) = q \bar{f}_1$  ( $q = k_2$  or  $k_1$ ). Eqs.(28,31,32) then relate  $\bar{f}_0$  and  $\bar{f}_1$  to  $\alpha, \beta, \delta$  as

$$\bar{f}_0 = \sin \delta e^{i\delta} \left( \frac{\alpha k_1}{k_2^2} - \frac{\beta k_2}{k_1^2} \right), \quad (39)$$

$$i \bar{f}_1 = \sin \delta e^{i\delta} \left( \frac{\alpha}{k_2^2} - \frac{\beta}{k_1^2} \right). \quad (40)$$

Thus the short-range behavior (Eqs.36,37) can be expressed in terms of  $\bar{f}_0, \bar{f}_1$  as (up to a prefactor  $4\pi \cot \delta$ )

$$\begin{aligned}\psi_0 &= \frac{i \bar{f}_1 (k_1^3 + k_2^3) - \bar{f}_0 (k_1^2 + k_2^2)}{k_2 - k_1} + \\ &\quad (i \bar{f}_1 (k_1 + k_2) - \bar{f}_0) \frac{\tan \delta}{r};\end{aligned}\quad (41)$$

$$\psi_1/i = \frac{i \bar{f}_1 (k_1^4 + k_2^4) - \bar{f}_0 (k_1^3 + k_2^3)}{3(k_2 - k_1)} r + i \bar{f}_1 \frac{\tan \delta}{r^2} \quad (42)$$

These results show that with SO coupling, the short-range parametrization of the wavefunction in each partial-wave channel will additionally depend on scattering amplitude of another partial-wave channel. This directly reflects the spin-mediated mixed scattering between different orbital (partial-wave) channels, as is one of the most dramatic features of SO coupled system.

At the end of this section, we study the bound state solution with energy  $E = -\kappa^2/m < 0$ . The bound state is given by the poles of scattering amplitudes ( $\bar{f}_0, \bar{f}_1 \rightarrow \infty$ ), which corresponds to the following transformation from the scattering state[2]

$$k \rightarrow i\kappa, \quad \delta \rightarrow -i\infty. \quad (43)$$

Using Eq.43, the bound state wavefunction can be deduced from Eq.33; its long-range and short-range behaviors can be deduced from Eqs.(34,35) and Eqs.(36,37) respectively.

### III. PSEUDO-POTENTIAL MODEL IN INDIVIDUAL PARTIAL-WAVE CHANNEL

The pseudo-potential model formulated in a given partial-wave channel is based on two assumptions. First, the interaction only acts on this particular channel. Second, the short-range behavior of wavefunction in this channel is still determined by the same scattering parameter as that in the absence of SO coupling. The second assumption is based on a general belief as follows. If the range of interacting potential ( $r_0$ ) is much shorter than any length scale in the system, as inter-particle distance approaches  $r \rightarrow r_0^+$ , all other potentials are negligible in this limit and the asymptotic behavior of two-body wavefunction is unchanged. The validity of pseudo-potentials has been verified in trapped systems in Ref.[2, 3, 5]. In the following we reduce the exact solutions obtained in Section II to the framework of s-wave and p-wave pseudo-potential models.

#### A. s-wave pseudo-potential

The s-wave pseudo-potential corresponds to assuming  $\bar{F}_1 = 0, \bar{f}_1 = 0$ ; by mapping the short-range behavior of  $\psi_0$ (Eq.41) to  $1/r - 1/a_s$  with  $a_s$  the s-wave scattering length in free space, we obtain the phase shift as

$$\tan \delta = -a_s \frac{\lambda^2 + k^2}{k}. \quad (44)$$

For scattering state, at low energies,  $\tan \delta = -a_s \lambda^2/k$  giving the effective 1D coupling  $g_{1D} = 2a_s \lambda^2/m$ , which is supported by the modified low-energy density of state(DOS) by isotropic SO couplings (see also Ref.[9]); at high energies, Eq.44 reduces to  $\tan \delta = -ka_s$  as in 3D free space.

The equation for bound state solution is obtained from Eq.44 via transformations as Eq.43,

$$-\frac{1}{a_s} \kappa = \lambda^2 - \kappa^2, \quad (45)$$

which reproduces the result obtained by s-wave T-matrix approach[9]. Eq.45 results in a bound state solution for arbitrarily weak interaction, which is a direct consequence of the effective 1D DOS at low energies.

#### B. p-wave pseudo-potential

The p-wave pseudo-potential corresponds to  $\bar{F}_0 = 0, \bar{f}_0 = 0$ , and  $\delta$  is determined by mapping the short-range behavior of  $\psi_1$ (Eq.42) to  $r/3 - v_p/r^2$ , with  $v_p$  the p-wave scattering volume in free space. We obtain

$$\tan \delta = -v_p \frac{\lambda^4 + 6\lambda^2 k^2 + k^4}{k}. \quad (46)$$

Without SO coupling ( $\lambda = 0$ ), it reproduces the original free space result as  $\tan \delta = -v_p k^3$ .

For scattering state at low energies,  $\tan \delta = -v_p \frac{\lambda^4}{k}$  again giving  $\delta(k=0) = \pi/2$ ; at high energies, it recovers the free space result.

For bound state, by transformation as Eq.43 we obtain from Eq.46 that

$$-\frac{1}{v_p} \kappa = \lambda^4 - 6\lambda^2 \kappa^2 + \kappa^4. \quad (47)$$

We see that for arbitrarily weak p-wave interaction  $v_p \rightarrow 0^-$ , Eq.47 gives a shallow bound state as  $\kappa = -v_p \lambda^4$ .

### IV. SCATTERING UNDER A SQUARE-WELL POTENTIAL AND VALIDITY OF PSEUDO-POTENTIALS

In this section we present the scattering state and bound state solutions under a square-well interaction potential. By comparing these solutions with those from individual s-wave and p-wave pseudo-potential model, we shall address the validity of pseudo-potentials in the presence of isotropic SO coupling. In Appendix A we show more details about partial-wave scattering under the square-well potential without SO coupling, and in Appendix B we derive the equations for two-body solutions with isotropic SO coupling.

#### A. Results

We consider a square-well potential with depth  $V_0 (< 0)$  at inter-particle distance  $r < r_0$  and with depth zero otherwise. The interaction strength is uniquely characterized by a dimensionless parameter as  $qr_0$ , with  $q = \sqrt{-mV_0}$ . Without SO coupling, Eq.A4 shows that by increasing  $qr_0$ , a sequence of s-wave resonances (with phase shift  $\delta_s = \pi/2$ ) occur at  $qr_0/\pi = n + 1/2$  and p-wave resonances ( $\delta_p = \pi/2$ ) at  $qr_0/\pi = n + 1$  ( $n = 0, 1, 2, \dots$ ). A bound state emerges whenever across a scattering resonance.

Next we solve the two-body problem in the presence of isotropic SO coupling. Based on exact solutions in section II, the wavefunctions inside the potential ( $r < r_0$ ) in orbital s-wave and p-wave channels are

$$\begin{aligned} \psi_0 &= j_0(q_2 r) + t j_0(q_1 r), \\ \psi_1/i &= j_1(q_2 r) + t j_1(q_1 r); \end{aligned} \quad (48)$$

with  $q_2 = \lambda + \sqrt{m(E - V_0)}$ ,  $q_1 = \lambda - \sqrt{m(E - V_0)}$ . Outside the potential ( $r > r_0$ ), the wavefunctions are given by Eq.33 for the scattering state ( $E = k^2/m > 0$ ), or by the transformed form (through Eq.43) for bound state ( $E = -\kappa^2/m < 0$ ).

Using the continuity properties of  $\psi_0$ ,  $\psi_1$  and their first-order derivatives at the boundary  $r = r_0$ , one can

solve all the unknown parameters  $\{t, \alpha, \beta, \delta\}$  for the scattering state and  $\{t, \alpha, \beta, \kappa\}$  for the bound state. In Appendix B we present the equations for these solutions. Next we show numerical results for the scattering state and bound state in turn.

### 1. Scattering state

For given energy  $E = k^2/m > 0$ , we obtain two phase shift solutions,  $\delta_1$  with  $\bar{f}_0 \gg \bar{f}_1$  and  $\delta_2$  with  $\bar{f}_1 \gg \bar{f}_0$ , analogous to s-wave and p-wave phase shifts without SO coupling. For fixed SO coupling  $\lambda r_0 = 0.2$ , we show in Fig.2(a) the solution of  $\delta_1$  near the first s-wave resonance and in Fig.2(b) the solution of  $\delta_2$  near the first p-wave resonance. Independently, we obtain  $\delta_1$  from Eq.44 using s-wave scattering length( $a_s$ ) with effective-range corrections (see Eq.A3,  $l = 0$ ), and  $\delta_2$  from Eq.46 using p-wave scattering length( $a_p \equiv v_p/r_0^2$ ) with effective-range corrections (Eq.A3,  $l = 1$ ). In Fig.2, these results are shown (by orange dashed lines) to compare with exact solutions (black circles).

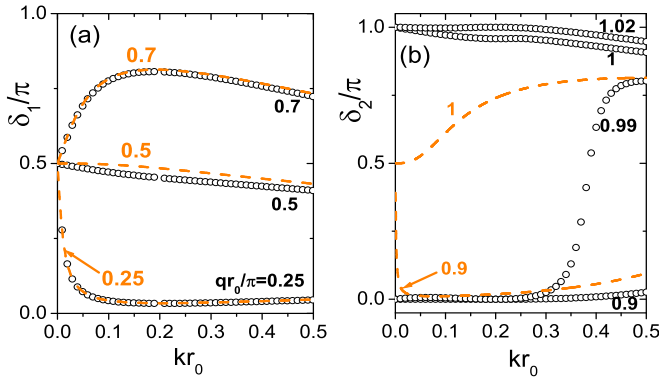


FIG. 2: (Color online) Phase shifts of scattering states in a square-well potential with isotropic SO coupling strength  $\lambda r_0 = 0.2$ . Exact solutions are shown (by black circles) in comparison with results from pseudo-potential models with effective-range corrections (see Eq.A3) (by orange dashed lines). (a)  $\delta_1$  near s-wave resonance with (from bottom to top)  $qr_0/\pi = 0.25$  ( $a_s < 0$ ),  $0.5$  ( $a_s = \infty$ ),  $0.7$  ( $a_s > 0$ ). (b)  $\delta_2$  near p-wave resonance with (from bottom to top)  $qr_0/\pi = 0.9$  ( $a_p < 0$ ),  $0.99$  ( $a_p < 0$ ),  $1$  ( $a_p = \infty$ ),  $1.02$  ( $a_p > 0$ ).

For the solution  $\delta_1$  near s-wave resonance, Fig.2(a) shows that it can be approximately fit by s-wave model within  $kr_0 < 0.5$ . Particularly at  $k = 0$ ,  $\delta_1 = \pi/2$  is consistent with the s-wave prediction (Eq.44) due to the 1D feature of the low-energy DOS. However, there is still a small deviation between these two solutions at finite  $k$ , due to the interplay between SO coupling, p-wave contribution and the finite potential range. To investigate these effects in detail, we further study the modified effective scattering length  $a_{eff}$  in s-wave channel, which is defined by  $\psi_0(r) \rightarrow 1/r - 1/a_{eff}(k)$  at  $r_0 < r \ll 1/k$ . Practically  $a_{eff}(k)$  can be extracted from the asymptotic

wavefunction (41) by diagonalizing Eq.B1 in Appendix B. Fig.3(a) shows how  $a_{eff}(k)$  evolves with  $k$  for each given SO coupling, which can also be expressed in the form of effective-range correction,

$$\frac{1}{a_{eff}(k)} = \frac{1}{a_{eff}} - \frac{1}{2}r_{eff}k^2. \quad (49)$$

One can see that with increased SO couplings, the effective range  $r_{eff}$  almost stay unchanged while  $1/a_{eff}$  become smaller indicating weaker interactions. The deviations of  $1/a_{eff}$  from  $1/a_s$  directly manifest the effect of SO coupling and mixed scattering of s-wave channel with p-wave channel. Moreover the mixing can also be seen from the additional dependence of  $\psi_0$  on the p-wave scattering amplitude in Eq.41. In Fig.3(b) we show the zero-energy value  $1/a_{eff}$  as a function of  $\lambda r_0$  for several different potential depths. At  $\lambda r_0 \ll 1$ ,  $1/a_{eff}$  can be well fit by

$$\frac{r_0}{a_{eff}} = \frac{r_0}{a_s} + C(\lambda r_0)^2, \quad (50)$$

where the dimensionless parameter  $C$  only depends on the properties of the potential, or the actual interaction strengths in s-wave and p-wave channels. In Fig.4,  $C$  is shown as a function of  $r_0/a_s$  (together with  $a_p/a_s$ ) near the first s-wave resonance. In the weak interaction limit,  $|V_0| \rightarrow 0$  and  $a_s, a_p \rightarrow 0^-$ ,  $C$  change linearly with  $r_0/a_s$ , indicating  $a_{eff} - a_s \propto -(\lambda r_0)^2$  in this limit. For the typical parameter regime in the present experiment[6],  $\lambda$  is determined by the wavevector of the laser which is much smaller than the cutoff momentum of realistic potential. In this case, the condition  $\lambda r_0 \ll 1$  gives negligible correction to  $a_{eff}$  near s-wave resonances.

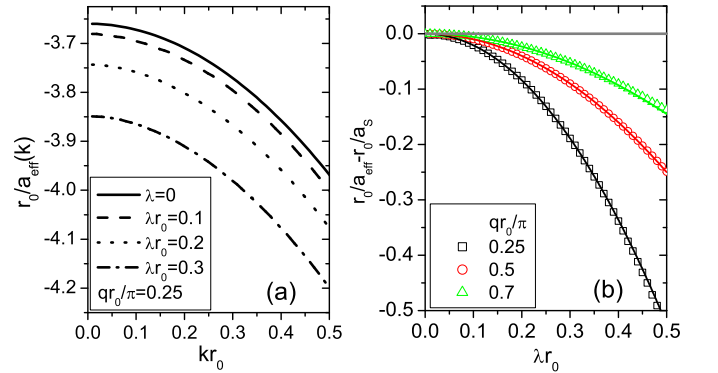


FIG. 3: (Color online) (a) Inverse of effective scattering lengths ( $a_{eff}(k)$ ) as functions of  $k$  for different SO couplings  $\lambda r_0 = 0, 0.1, 0.2, 0.3$  (from top to bottom). The potential depth is  $qr_0/\pi = 0.25$ . (b) Inverse of zero-energy scattering lengths ( $a_{eff}$ ) as functions of  $\lambda$  at different  $qr_0/\pi = 0.25, 0.5, 0.7$  (from bottom to top). The lines are fits to Eq.50 with  $C = -2.10, -1.00, -0.58$  (from bottom to top).

For the solution  $\delta_2$  near p-wave resonance, however, it behaves qualitatively different from that obtained

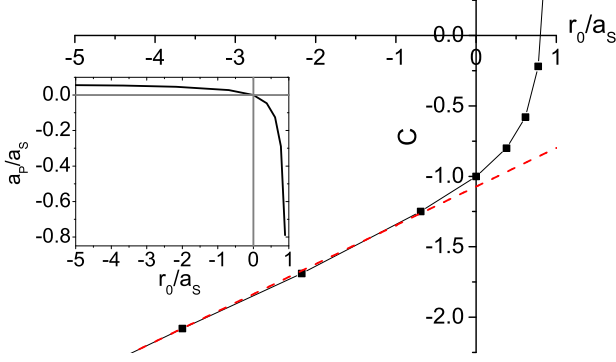


FIG. 4: (Color online)  $C$  in Eq.50 as functions of  $r_0/a_s$  near and across the first s-wave resonance ( $qr_0 < \pi$ ) in the square-well potential. The red dashed line is the linear fit in the weak interaction limit as  $C = -1.073 + 0.275r_0/a_s$ . Inset shows the ratio of p-wave to s-wave scattering length, where the gray (light) lines denote the s-wave resonance.

entirely in the framework of p-wave pseudo-potential model, as showed by Fig.2(b). Obviously, the exact solution shows the initial value  $\delta_2(k=0) = 0$  or  $\pi$ , depending on whether or not there is a two-body bound state (see next section); while the p-wave model always predicts  $\delta_2(k=0) = \pi/2$  according to Eq.46. We have checked that in the limit of  $\lambda r_0 \ll 1$ , the exact solution of  $\delta_2$  at  $k \ll 1/r_0$  essentially follows the free space result (given by  $\tan \delta_2 = -v_p k^3$ ) with  $\delta_2 \sim 0$  or  $\pi$ ; while the p-wave model gives a narrow momentum window as  $0 < k < \lambda$  when  $\delta_2(k)$  evolves from  $\pi/2$  to the exact result. This dramatic difference indicates that even near the p-wave resonance, the p-wave pseudo-potential alone can not be applied to the fermion system if  $\lambda$  is larger or comparable to the Fermi momentum. We shall analyze the reason for the breakdown of p-wave model to scattering state solutions in the discussion section.

## 2. Bound state

The bound state solution  $E = -\kappa^2/m < 0$  is given by the transformed matrix equation  $|A_b| = 0$  (see Appendix B). By setting  $\kappa = 0$  in the matrix equation we determine the critical potential depth  $|V_0|_c$ , which is responsible for the emergence of a new bound state, by

$$j_0(q_2 r_0) j_1(q_1 r_0) = j_0(q_1 r_0) j_1(q_2 r_0), \quad (51)$$

with  $q_2 = \lambda + q_c$ ,  $q_1 = \lambda - q_c$  and  $q_c = \sqrt{m|V_0|_c}$ . The solution of  $q_c$  is shown in Fig.5. As  $\lambda$  approaches zero, one branch of solution (solid line) is given by  $j_1(q_c r_0) = 0$  or  $a_s = 0$ ; the other branch (dashed line) is given by  $j_0(q_c r_0) = 0$  or  $a_p = \infty$ . For the first branch, when increasing  $\lambda$  the lowest solution will stay at  $q_c r_0 = 0$  or  $a_s = 0^-$ , while the other solutions increase resulting in deeper potential depths. For the second branch, when increasing  $\lambda$  all solutions of  $q_c$  will decrease, implying that

weaker interaction is required to support the new bound state near p-wave resonance. In all, we see that only the lowest solution of the first branch is consistent with the prediction from s-wave pseudo-potential model (see Eq.45), but none of the other solutions. The discrepancies here are attributed to the mixed scattering between s-wave and p-wave channels induced by the isotropic SO coupling.

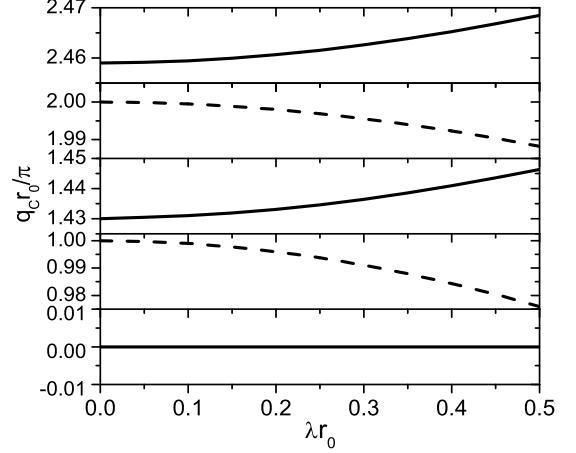


FIG. 5: Critical potential depth ( $q_c r_0 / \pi$ ) for the emergence of each new bound state as a function of isotropic SO coupling strength. When  $\lambda r_0 \rightarrow 0$ , the solid lines approach  $q_c r_0 / \pi = 0, 1.430, 2.459, \dots$  with  $a_s = 0$ ; the dashed lines approach  $q_c r_0 / \pi = 1, 2, \dots$  with  $a_p = \infty$  (See text).

As shown in Fig.6 with fixed  $\lambda r_0 = 0.2$ , a sequence of bound states will develop when the potential depths increase above critical  $|V_0|_c$ . For comparison, we also present the results from s-wave and p-wave pseudo-potential models, using the scattering length with or without energy-dependence. (For the bound state, the energy-dependent scattering length is determined from Eqs.(A2,A4) but with  $k$  replaced by  $i\kappa$ . [2])

Fig.6(a) shows that the s-wave model using s-wave scattering length without ( $a_s$ ) or with ( $a_s(E)$ ) energy-dependence both give good approximations to low-energy solutions near s-wave resonance, but deviate a lot from exact solutions for deep bound states. In general, we find that using  $a_s(E)$  provides more accurate results than using  $a_s$  in a large energy-range; particularly, in the limit of zero SO coupling, using  $a_s(E)$  will give the exact bound state solutions [2]. For fixed potential depth, the deviation of s-wave results from exact solutions increases with the SO coupling strength, as shown in Fig.7(a1,a2). Moreover, Fig.6(a) and Fig.7 show that the s-wave models using  $a_s(E)$  always predict deeper bound states than real solutions, which is consistent with Eq.50 and also Fig.3 that the presence of SO coupling reduces the effective interaction parameter for low-energy states.

In Fig.7(b), we further plot the relative deviations,  $\Delta\kappa/\kappa$ , as functions of SO coupling strengths at different potential depths. It shows that  $\Delta\kappa/\kappa$  increases



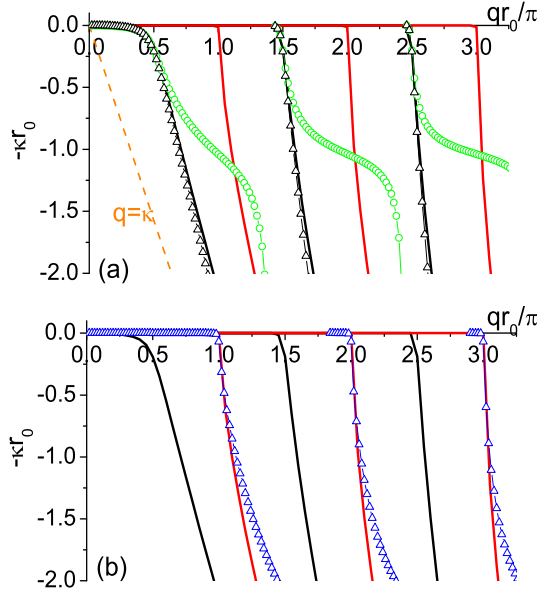


FIG. 6: (Color online) Bound state solutions (solid lines) in the square-well potential as functions of the potential depths, in comparison with results from s-wave(a) and p-wave(b) pseudo-potential models. The SO coupling is  $\lambda r_0 = 0.2$ . In (a), we have used s-wave scattering length without (green circles) or with (black triangles) energy-dependence. In (b), we use the energy-dependent p-wave scattering length (blue triangles).

more rapidly for deep bound states than that for shallow ones. As also mentioned in the introduction, the s-wave model (even using the energy-dependent  $a_s(E)$ ) is quite questionable when applied to deep molecules. As shown in Fig. 8, the energy of the bound state is always lower bounded by the potential depth  $V_0$ , i.e.,  $\kappa < q$ . However, the s-wave model will produce unphysically deep molecules with  $\kappa > q$ . In this case, the s-wave model alone will not work and one must take into account the effect mixed scattering with p-wave channel due to SO couplings.

In Fig. 6(b) we show the comparison with results from p-wave pseudo-potential model. According to the p-wave model (see Section III B), the bound state exists for an arbitrarily weak interaction in the presence of isotropic SO coupling. This is qualitatively different from the exact solution under the square-well potential, where each emergence of a new bound state requires a potential depth beyond the critical value (as shown by red lines in Fig. 5). In the limit of  $\lambda r_0 \ll 1$ , the critical depths continuously approach  $q_c r_0 / \pi = 1, 2, \dots$  as in free space. The breakdown of p-wave model to bound state solutions will be discussed in the following section.

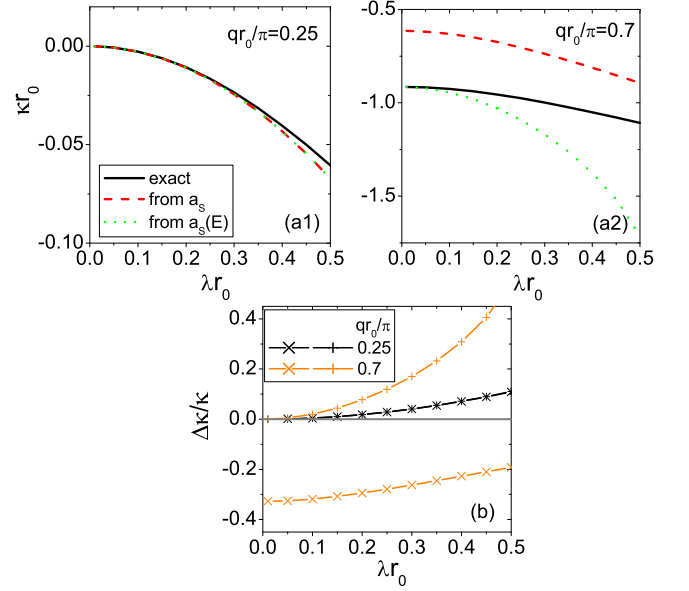


FIG. 7: (Color online) (a1,a2) Bound state solutions in a square-well potential as functions of isotropic SO coupling strengths at potential depths  $qr_0/\pi = 0.25$  [(a1),  $a_s < 0$ ] and  $0.7$  [(a2),  $a_s > 0$ ], in comparison with results using s-wave scattering length without (red dashed line) or with (green dot line) energy-dependence. (b) Relative deviations between exact solutions and results from s-wave pseudo-potential model, at the same potential depths as in (a1,a2). For s-wave pseudo-potential, we use s-wave scattering length without (' $\times$ ') or with ('+') energy-dependence.

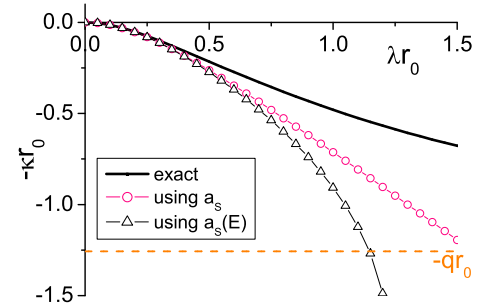


FIG. 8: (Color online) Bound state solutions as functions of isotropic SO coupling strengths for given potential depth  $qr_0/\pi = 0.4$ , in comparison with results using s-wave scattering length without (pink circles) or with (black triangles) energy-dependence. The orange dashed line denotes the lower bound as  $\kappa = q$ .

## B. Discussion

Through the last subsection, we have shown that the SO coupling has different effects on the validity of pseudo-potentials in s-wave and p-wave channels. In the limit of  $\lambda r_0 \ll 1$ , the s-wave pseudo-potential model provides good approximations to the low-energy scattering state and bound state solutions near s-wave resonances.



For example, it predicts correctly the initial phase shift as  $\delta_1(k=0) = \pi/2$  for scattering state, and a bound state solution for arbitrarily weak attraction  $a_s \rightarrow 0^-$ . However, near p-wave resonances the p-wave pseudo-potential will produce qualitatively different results compared with exact solutions. For example, in the limit of  $\lambda r_0 \ll 1$ , the exact solutions approach free space results, i.e.,  $\delta_2(k=0) = 0$  or  $\pi$ , and each bound state emerges when  $v_p$  goes across a resonance at certain critical potential depth; on the contrary, the p-wave model predicts  $\delta_2(k=0) = \pi/2$  and a bound state for any weak p-wave interaction  $v_p \rightarrow 0^-$ .

Here we analyze the reason why the s-wave pseudo-potential is approximately valid for SO coupled system while p-wave is not. This can be explained from the correspondence between the assumptions of pseudo-potential models and the resulted short-range behavior of wavefunctions. For s-wave pseudo-potential ( $\bar{f}_0 \neq 0$ ,  $\bar{f}_1 = 0$ ), the resulted wavefunction does not show  $1/r^2$  singularity in p-wave channel, which is consistent with the assumption of zero scattering amplitude in Eq.25. However, the p-wave pseudo-potential ( $\bar{f}_0 = 0$ ,  $\bar{f}_1 \neq 0$ ) will induce an additional singularity in s-wave channel, i.e.,  $\psi_0(r) \rightarrow 2\lambda[\frac{\lambda^2+3k^2}{2k} + \frac{\tan\delta}{r}]$  as  $r \rightarrow 0$ . This in turn requires that the interaction operator  $U$  also generate scattering amplitude in the s-wave channel, contradictory with the initial assumption that  $\bar{f}_0 = 0$  in Eq.25. This paradox also implies that any weak  $\bar{f}_0$  will have dramatic interference with the p-wave sector and lead to qualitatively different results from those using pseudo-potential entirely in p-wave channel.

The results presented in this section tell us that the original pseudo-potentials formulated in the absence of SO coupling do not necessarily apply to the case with SO coupling. The pseudopotential model will certainly breakdown if the results obtained are inconsistent with initial assumptions of this model. In this case, an appropriate interaction model should be constructed in order to rightly incorporate mixed scatterings between different partial-wave channels, which is out of the scope of this paper.

## V. SUMMARY

In this paper, we exactly solve the two-body problem of spin-1/2 fermions with isotropic SO coupling under a general short-range interaction potential, and investigate the validity of s-wave and p-wave pseudo-potentials formulated in the absence of SO couplings. Our main results are summarized as follows:

(1) In the presence of isotropic SO coupling, the two-body scattered wavefunction exhibits exotic dependences on the momentum and phase shift (Eq.33). In each partial-wave channel the wavefunction at short inter-particle distance is parameterized by scattering amplitudes of all coupled scattering channels (Eqs.41,42). This feature reveals the mixed scattering between different

partial-waves that is induced by the SO coupling.

(2) Under the conditions that the length scale of SO coupling much longer than the range of the potential ( $\lambda r_0 \ll 1$ ) and near s-wave resonances, the s-wave pseudo-potential gives a good approximation to the low-energy solutions, with the correction depending on the strength of SO coupling, the finite range of the potential and contributions from other coupled partial-waves.

(3) Near the p-wave resonance, the p-wave pseudo-potential model gives low-energy solutions that are qualitatively different from the exact ones from the square-well potential. The p-wave model alone can not be applied to the fermion system when the SO coupling strength is larger or comparable to the Fermi momentum. Its breakdown is attributed to the inconsistent treatment between the assumption of the p-wave pseudo-potential and the resulted short-range singularities of wavefunction in s-wave channel.

Although above results are obtained for the special type of isotropic SO coupling, they reveal the generic scattering properties modified by the coupling between spin and orbit. We therefore expect these results have strong implications to other systems with a general type of SO coupling.

*Acknowledgement.* The author is grateful to T.-L. Ho and H. Zhai for valuable discussions, and to P. Zhang and S. Zhang for helpful suggestions. This work is supported by Tsinghua University Basic Research Young Scholars Program and Initiative Scientific Research Program and NSFC under Grant No. 11104158.

## Appendix A: Free-space scattering lengths under a square-well potential

Far away from the range ( $r_0$ ) of the potential, the scattered wavefunction in  $l$ -th partial-wave channel reads

$$\psi_l(r) = j_l(kr) - \tan \delta_l n_l(kr) \quad (\text{A1})$$

here  $\delta_l$  is the phase shift which give the scattering length (with energy-dependence) as

$$a_l(k) = -\frac{1}{r_0^{2l}} \frac{\tan \delta_l}{k^{2l+1}}. \quad (\text{A2})$$

In the limit of  $kr_0 \ll 1$ , the effective-range expansion gives

$$\frac{1}{a_l(k)} = \frac{1}{a_l} - \frac{1}{2} r_l k^2, \quad (\text{A3})$$

with  $a_l$  the zero-energy scattering length and  $r_l$  the effective range.

For a square-well potential with depth  $V_0 (< 0)$  and range  $r_0$ , in the following we scale all lengths ( $a_l, r_l$ ) in the unit of  $r_0$  and all momenta ( $k, p$ ) of  $1/r_0$ ; for instance,  $\tilde{a} = a/r_0$ ,  $\tilde{k} = ka_0$ . We define two functions as  $\tilde{j}_l(x) = x^{-l} j_l(x)$ ,  $\tilde{n}_l(x) = x^{l+1} n_l(x)$ , modified respectively from

the spherical Bessel and Neumann functions. We then have

$$\frac{\tan \delta_l}{\tilde{k}^{2l+1}} = \frac{\bar{j}_{l-1}(\tilde{p})\bar{j}_l(\tilde{k}) - \bar{j}_{l-1}(\tilde{k})\bar{j}_l(\tilde{p})}{\bar{j}_{l-1}(\tilde{p})\bar{n}_l(\tilde{k}) - \bar{n}_{l-1}(\tilde{k})\bar{j}_l(\tilde{p})} \quad (\text{A4})$$

with  $k = \sqrt{mE}$ ,  $p = \sqrt{m(E - V_0)}$ . Note that for  $l = 0$ , we have  $j_{-1} = -n_0$ ,  $n_{-1} = j_0$ . The zero-energy scattering length and effective range are given by ( $q = \sqrt{-mV_0}$ )

$$\begin{aligned} \tilde{a}_l &= -\frac{1}{(2l-1)!!(2l+1)!!} \frac{j_{l+1}(\tilde{q})}{j_{l-1}(\tilde{q})}, \\ \tilde{r}_l &= (2l-1)!!(2l+1)!! \left\{ -\frac{1}{2l-1} + \frac{2l+1}{\tilde{q}^2} \frac{j_{l-1}(\tilde{q})}{j_{l+1}(\tilde{q})} \right\} \end{aligned} \quad (\text{A5})$$

$$-\frac{1}{2l+3} \left( \frac{j_{l-1}(\tilde{q})}{j_{l+1}(\tilde{q})} \right)^2 \}. \quad (\text{A6})$$

### Appendix B: Scattering under a square-well potential with isotropic SO coupling

Using the continuity properties of  $\psi_0$ ,  $\psi_1$  and their first-order derivatives at the potential boundary  $r = r_0$ , we obtain four coupled equations which can be expressed in a matrix form. For convenience, we scale all momenta in unit of  $1/r_0$  as  $\tilde{k} = ka_0$ .

For scattering state ( $E = k^2/m > 0$ ), the matrix equation is  $A(1, t, \alpha, \beta)^T = 0$  with matrix

$$A = \begin{pmatrix} j_0(\tilde{q}_2) & j_0(\tilde{q}_1) & j_0(\tilde{k}_2) - \tan \delta n_0(\tilde{k}_2) & j_0(\tilde{k}_1) + \tan \delta n_0(\tilde{k}_1) \\ \tilde{q}_2 j_1(\tilde{q}_2) & \tilde{q}_1 j_1(\tilde{q}_1) & \tilde{k}_2(j_1(\tilde{k}_2) - \tan \delta n_1(\tilde{k}_2)) & \tilde{k}_1(j_1(\tilde{k}_1) + \tan \delta n_1(\tilde{k}_1)) \\ j_1(\tilde{q}_2) & j_1(\tilde{q}_1) & j_1(\tilde{k}_2) - \tan \delta n_1(\tilde{k}_2) & j_1(\tilde{k}_1) + \tan \delta n_1(\tilde{k}_1) \\ \tilde{q}_2 j_0(\tilde{q}_2) & \tilde{q}_1 j_0(\tilde{q}_1) & \tilde{k}_2(j_0(\tilde{k}_2) - \tan \delta n_0(\tilde{k}_2)) & \tilde{k}_1(j_0(\tilde{k}_1) + \tan \delta n_0(\tilde{k}_1)) \end{pmatrix} \quad (\text{B1})$$

here we have used  $j'_0(x) = -j_1(x)$ ,  $j'_1(x) = -\frac{2}{x}j_1(x) + j_0(x)$  to simplify the equations.  $k = \sqrt{mE}$ ,  $q = \sqrt{-mV_0}$ ;  $k_2 = \lambda + k$ ,  $k_1 = \lambda - k$ ;  $q_2 = \lambda + \sqrt{k^2 + q^2}$ ,  $q_1 = \lambda - \sqrt{k^2 + q^2}$ .

The zero determinant  $|A| = 0$  gives rise to two solutions of phase shift  $\delta$ . When  $\lambda = 0$ , these two solutions are respectively resulted from two decoupled equations, and reproduce the well-known s-wave and p-wave phase

shifts in free space as given by Eq.A4.

For bound state, the equations can be obtained straightforwardly by transformations (see Eq.43) from the equations of scattering state. The binding energy  $E = -\kappa^2/m < 0$  can be determined from the resulted matrix equation  $|A_b| = 0$ . When  $\lambda = 0$ , the binding energies respectively reproduce the s-wave and p-wave results without SO coupling.

- 
- [1] K. Huang and C. N. Yang, Phys. Rev. **105**, 767 (1957).
  - [2] R. Stock, A. Silberfarb, E. L. Bolda and I. H. Deutsch, Phys. Rev. Lett. **94**, 023202 (2005).
  - [3] D. Blume and C. H. Greene, Phys. Rev. A, **65**, 043613(2002); E. L. Bolda, E. Tiesinga and P. S. Julienne, Phys. Rev. A **66**, 013403 (2002),
  - [4] V. Gurarie and L. Radzihovsky, Annals of Physics, **322**, 2 (2007).
  - [5] S.-K. Yip, Phys. Rev. A **78**, 013612 (2008); S.-G. Peng, S.-Q. Li, P. D. Drummond and X.-J. Liu, arXiv:1107.2740.
  - [6] Y. J. Lin, R. L. Compton, A. R. Perry, W. D. Phillips, J. V. Porto and I. B. Spielman, Phys. Rev. Lett. **102**, 130401 (2009); Y. J. Lin, R. L. Compton, K. Jimnez-Garcia, J. V. Porto and I. B. Spielman, Nature **462**, 628 (2009); Y.-J. Lin, K. Jimnez-Garcia and I. B. Spielman, Nature **471**, 83 (2011).
  - [7] D. L. Campbell, G. Juzeliūnas and I. B. Spielman, arXiv: 1102.3945; J. D. Sau, R. Sensarma, S. Powell, I. B. Spielman and S. Das Sarma, Phys. Rev. B **83**, 140510(R) (2011); Z. F. Xu and L. You, arXiv: 1110.5705.
  - [8] H. Zhai, Int. J. Mod. Phys. B **26**, 1230001 (2012).
  - [9] J. P. Vyasankere and V. B. Shenoy, Phys. Rev. B **83** 094515 (2011); J. P. Vyasankere and V. B. Shenoy, arXiv:1108.4872.
  - [10] E. L. Bolda, E. Tiesinga and P. S. Julienne, Phys. Rev. A **68**, 032702 (2003); K. Kanjilal and D. Blume, Phys. Rev. A **70**, 042709 (2004).
  - [11] Y. Nishida and S. Tan, Phys. Rev. A **82**, 062713 (2010).
  - [12] J. R. Taylor, *Scattering theory* (Wiley, New York, 1972).